Journal of Atmospheric and Solar-Terrestrial Physics 142 (2016) 20–24

Contents lists available at ScienceDirect

Journal of Atmospheric and Solar-Terrestrial Physics

journal homepage: www.elsevier.com/locate/jastp

Orientation variation of dayside auroral arc alignments obtained from all-sky observation at yellow river station, Svalbard

Qi Qiu [a,b,*], Hui-Gen Yang [b,**], Quan-Ming Lu [a], Ze-Jun Hu [b], De-Sheng Han [b], Qian Wang [c]

[a] CAS Key Laboratory of Geoscience Environment, Department of Geophysics and Planetary Science, University of Science and Technology of China, Hefei, China
[b] SOA Key Laboratory for Polar Science, Polar Research Institute of China, Shanghai, China
[c] School of Telecommunication and information Engineering, Xi'an University of Posts and Telecommunications, Xi'an, China

ARTICLE INFO

Article history:
Received 30 September 2015
Received in revised form
23 February 2016
Accepted 25 February 2016
Available online 26 February 2016

Keywords:
Dayside auroral arc
The orientation of arc alignment
Arc tilt

ABSTRACT

The orientations of dayside auroral arc alignments were calculated for over 40,000 images from all-sky observation at Yellow River Station, Svalbard. For each arc, its "orientation" and "tilt" are defined as the angle the arc alignment makes with the dusk-dawn direction and the local east-west direction, respectively. The mean arc orientation increases linearly with the increasing magnetic local time (MLT). There is a reversal point of the arc tilt located at near 10.5 MLT. Compared with the mean orientation, auroral arc alignment tilts to morning side in the higher latitude and tilts to evening side in the lower latitude in the prenoon sector, whereas it is the opposite in the postnoon sector. We further studied the effects of the interplanetary magnetic field (IMF) on the location of the arc tilt reversal point. We found that the reversal position shifts toward the midday for negative B_y.

1. Introduction

The aurora is one of the important phenomena in the solar-terrestrial environment. The auroral oval (Feldsten, 1963; Feldsten and Starkov, 1967) appears as a continuous ring of emissions encircling the geomagnetic pole (Liou et al., 1997). There exist two distinctive auroral emission regions in the auroral oval: nightside region centered at 2230 magnetic local time (MLT) and 68 magnetic latitude (MLAT), dayside region centered at both 1500 MLT and 75 MLAT and 1000 MLT and 75 MLAT (Liou et al., 1997). These auroral emission regions are consistent with probability of the electron acceleration events (Newell et al., 1996). An auroral arc is the basic form of discrete aurora, the brightest and most obvious kind of aurora (Davis, 1978). The precipitating particle of auroral arc is accelerated in the magnetoshpere-ionosphere system (Borovsky, 1993).

An earlier study by Hultqvist (1962) showed the mean orientation of arcs during the hours around midnight approximately parallel to the lines of constant corrected geomagnetic latitude. Later, Lassen and Danielsen (1978) utilized quiet time arcs observed from the Greenland all-sky camera network to establish a relationship between interplanetary magnetic field (IMF) orientation and arc location. They distinguished the discrete quiet arcs into two types: the first type, which is dominant when B_z is negative, is oriented along the statistical auroral oval; the second type, which is prominent when B_z is positive, is ordered in the sun-earth direction over the polar cap. We are more interested in the first type of discrete arcs in this study. Recently, Gillies et al. (2014) used data from the THEMIS All-Sky Image array to survey the quiet auroral arc orientation. They determined the "tilt" to be the angle the arc makes with the local magnetic east-west direction and found that the arc tilt reversal point is on average prior to magnetic midnight.

The previous study however was focused on the nighttime discrete aurora, dayside auroras were studied more and more in the recent year. Sandholt et al. (2002) divided dayside auroral forms in to 6 types using meridian scanning photometer (MSP) and all-sky cameras from Ny-Ålesund, Svalbard. The type 1 aurora is poleward moving auroral forms (PMAFs), which is generally located in the magnetic latitude region 70°–75° in the midday sector. The type 2 aurora is the midday aurora located within 75°–80° MLAT when the IMF is northward. It is characterized by a sequence of poleward boundary intensifications. The type 3 is diffuse aurora, which is located on the equatorward side of the type 1 forms in the prenoon sector. The auroral forms of types 4 and 5 are the prenoon and postnoon multiple arcs. The type 6 auroral forms are polar cap arcs, which is called sun-aligned arcs.

* Corresponding author at: CAS Key Laboratory of Geoscience Environment, Department of Geophysics and Planetary Science, University of Science and Technology of China, Hefei, China.
** Corresponding author.
E-mail addresses: qiuqi@pric.org.cn (Q. Qiu), huigen_yang@pric.org.cn (H.-G. Yang).

http://dx.doi.org/10.1016/j.jastp.2016.02.019
1364-6826/

This study is focused on the auroral forms of types 4 and 5. Kozlovsky and Kangas (2002) found poleward moving auroral arcs (PMAAs) are observed on closed magnetic field lines in the midday sector, which is different from PMAFs. Some arcs in the midday sector were also investigated in this study.

This study quantified the orientation of stable dayside auroral arcs. The stable arcs are elongated in longitude and narrowed in latitude. The lengths of auroral arcs are 100–1000 km (Davis, 1978). The widths of arcs are less than 100 km, having an average value of 18.5 km (Qiu et al., 2013). In total there were 42493 images identified that contained the stable auroral arcs, of which 23135 contained single arcs and the other 19358 contained multiple arcs. The variations of arc orientations were investigated in magnetic latitude (MLAT) and longitude, and the effects of the IMF conditions were discussed.

2. Data and methodology

The data used in this study were collected during 0600–1800 MLT from December 2003 to February 2007 with the all-sky camera (ASC) at Chinese Yellow River Station (YRS), at Ny-Ålesund, Svalbard. YRS is located at 78.92 °N in the geographic latitude or 76.24° MLAT, and MLT ≈ UT + 3 h (Hu et al., 2009). This station is at the cusp latitude, which is suitable to observe dayside aurora. The camera uses a 512 × 512 square pixel array, and the center of the field of view is geographic zenith. All-sky images (ASIs) are taken with a 7 s exposure time at 10 s cadence, using a 557.7 nm filter having a bandwidth of 2 nm.

In an ASI, every pixel has the same solid angle. Using trigonometric relations, the distance d away from the zenith and geocentric angle a varied with the corresponding zenith angle (ZA) θ is given as (Qiu et al., 2013)

$$a = \theta - \sin^{-1}\left[\frac{R_E}{R_E + h}\sin\theta\right] \quad (1)$$

$$d = (R_E + h) \times a \quad (2)$$

Where R_E is the earth radius and h is the altitude of aurora emission. Using (Eqs. (1) and 2), we can find the distance d varies approximately linearly with ZA as it is less than 60°, but it becomes an exponential relationship when ZA is larger than 60°. We just considered the arcs whose ZA is less than 60° in this study. The single-pixel spatial resolution is 1.1 km above zenith (at 150 km) and it increases to 3.9 km at 60° of ZA, having an average value of 1.7 km. The arcs are located between 74.1 MLAT and 78.3 MLAT as their ZAs are in the range of ± 60°. The ZA is positive as the arc is located poleward of zenith.

For each arc ASI, we first traced out the skeleton of the arc to represent its alignment. Then, we converted the points in the skeleton into a geomagnetic coordinate and performed a simple linear regression. At last, we mapped them into the MLT-MLAT coordinate to determine the orientation of the arc. Fig. 1a shows an example of an auroral arc in an ASI (obtained on 24 December 2003 at 13:59:31 UT). The arc captured within the field of view is only part of a much longer arc, which appears in the majority of ASIs. The solid blue line is the magnetic meridian. We can draw an intensity variation curve by extracting along the magnetic meridian, which is shown by solid blue line in Fig. 1b). An arc is

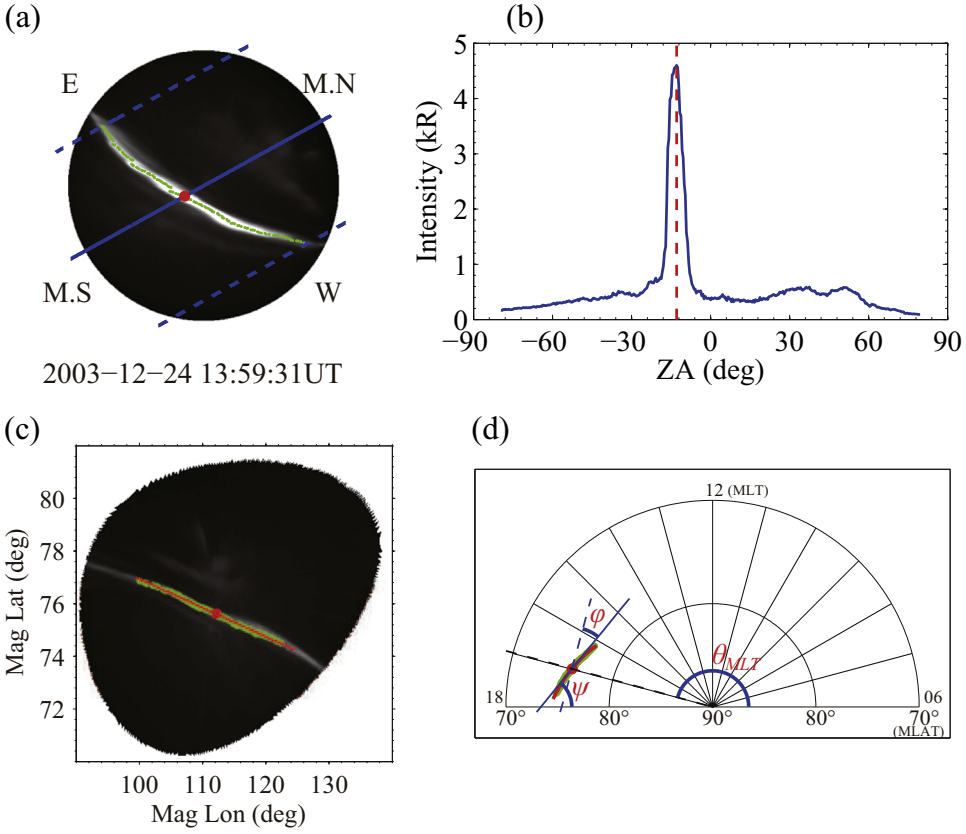

Fig. 1. (a) Arc image with an all-sky camera (5577 Å) taken at YRS, December 24, 2003, at 13:59:31 UT. The solid blue line is along the magnetic meridian and the dashed blue line is the parallel of this line at 60° of ZA. The red point is located at an arc and the green blobs represent the arc alignment. (b) Intensity as a function of ZA along the magnetic meridian. (c) The arc from (a) converted into a geomagnetic coordinate reference frame. The fitted line is plotted in red. (d) The arc converted into the MLT-MLAT coordinates. The magnetic local east-west direction is shown by the dashed blue line. (For interpretation of the references to color in this figure legend, the reader is referred to the web version of this article.)

corresponding to a peak in this curve and it is located at the ZA of the peak, which is labeled with the dashed red line in Fig. 1b. The skeleton of an arc, which is shown by the green blobs, can be obtained using the same method along the lines parallel to magnetic meridian. A stable auroral arc requires the number of the points in the skeleton of the arc to be greater than 70, which results in the length of an arc larger than 100 km. Before we determine the orientation of the arc, we converted the location of these points from the CCD reference frame to geomagnetic coordinates, which are marked by green blobs in Fig. 1c. The solid red line is a fit of these points in geomagnetic coordinates. In order to determine the arc orientation easily, we map the fitted line to MLT-MLAT coordinates, as shown in Fig. 1d. The orientation of an arc ψ, which is defined as the angle between the alignment of auroral arc and the dusk-dawn direction, is the angle corresponding to the tangent slope of this fitted line at the location of the arc. The tilt of an arc φ, referred from Gillies et al. (2014), is defined as the angle between the arc alignment and the local east-west direction. Arc tilt is positive if the east part of the arc alignment is in the north of the magnetic local east-west direction. The relationship between arc tilt φ and arc orientation ψ is satisfied as

$$\phi = 90^\circ + \psi - \theta_{MLT}, \quad -90^\circ \le \phi, \quad \psi \le 90^\circ \tag{3}$$

$$\theta_{MLT} = (MLT - 6) \times 15^\circ, \quad 6 \le MLT \le 18 \tag{4}$$

The arc is located at the red point in Fig. 1d. The solid blue line is the tangent line of the fitted line at the location of the arc, and the dashed blue line points in the magnetic local east-west direction. Arc tilt φ in this example is negative. From Fig. 1d, the arc was located at about 78 MLAT at 1600 MLT. It was located in the lower latitude (75 MLAT) when the MLT increased to 1730 MLT. The tilt of auroral arc is equatorward (poleward) as it is negative (positive).

3. Result and discussion

The orientation can be determined for any arcs. For multiple-arc system, the orientation of each arc in an ASI was calculated separately. Fig. 2a is the scatter plot of the orientations for 67969 auroral arcs as a function of MLT. The number of arcs near magnetic midday (1030–1330 MLT) is less (only 2707) because of midday gap (Cogger et al., 1977). The solid green line is the fitted line with the correlation coefficient of 0.96 and the standard deviation σ of 11.2° respectively. The mean (fitted) value of arc orientations increases from −70.4° at 06 MLT to 53.5° at 18 MLT. Taking arc orientation into (Eqs. (3) and 4), Fig. 2b shows the scatter plot of arc tilt as a function of MLT. The green lines are the same as those in Fig. 2a. We can see a clear trend that arc tilt is decreased with the increasing MLT gradually and it is reversed in this process. The mean tilts are 19.5° at 0600 MLT and −36.6° at 1800 MLT, respectively. The average reversal position labels at the point where the fitted line crosses zero, which is marked by red 'X' at 10.2 MLT in Fig. 2b.

In order to further investigate the reversal of arc tilt, the reverse rate R is defined as

$$R = \frac{\min\{N_a, N_b\}}{\max\{N_a, N_b\}} \tag{5}$$

N_a is the number of arc tilts above zero and N_b is the number of arc tilts below zero. It is called as "the poleward reverse rate" if $N_a > N_b$, which means the poleward arc tilt is dominant at that time, otherwise "the equatorward reverse rate". Fig. 2c shows a distribution of the reverse rate of arc tilt as a function of MLT. Because arcs occur infrequently around the midday, each bin of distribution is taken from data within 30 min of MLT from 10.5 to 13.5 MLT, whereas it is taken within 10 min at the other time. Thus, the error of the reversal position is 30 min between 10.5 and 13.5 MLT and the error is 10 min at the other time. The poleward reverse rate is plotted with solid blue line and the equatorward one is plotted with dashed blue line. There is a clear demarcation point plotted with the vertical red line at 10.5 MLT where the distribution curve turning from solid to dashed. Here it is the position of the reversal point, which approximates that obtained in Fig. 2b. If the number of sample is large enough and the segmentation of distribution is fine enough, the reverse rate is equal to 1.0 at the reversal point. We can see the peak of distribution is just before the reversal point and the peak value is close to 1 (0.83) in Fig. 2c. Separate analyzing the tilts for single-arc ASIs or for multiple-arc systems (not shown), arc reversal still occurs at near

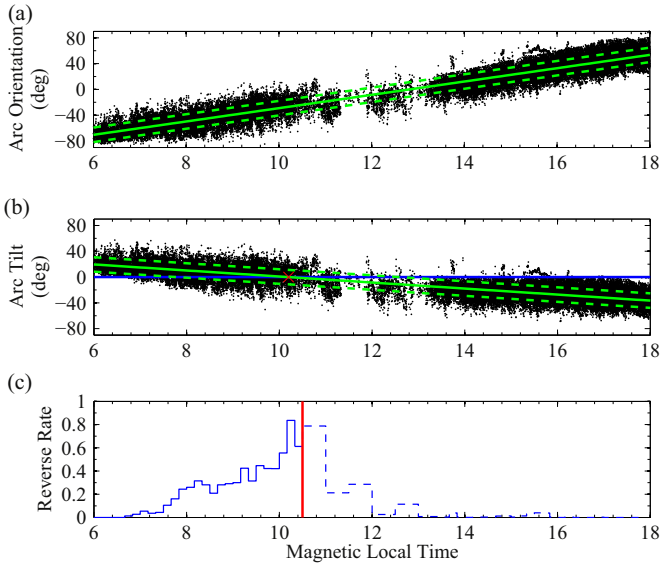

Fig. 2. (a) Arc orientation and (b) Arc tilt as a function of MLT. Best fit linear regression lines plotted with solid green lines and ± 1 σ deviation from linear regression line plotted with dashed green line. (c) Distribution of arc tilt reverse rate as a function of MLT. The poleward (equatorward) reverse rate is ploted with solid (dashed) line. The vertical red line represents the arc tilt reversal position. (For interpretation of the references to color in this figure, the reader is referred to the web version of this article.)

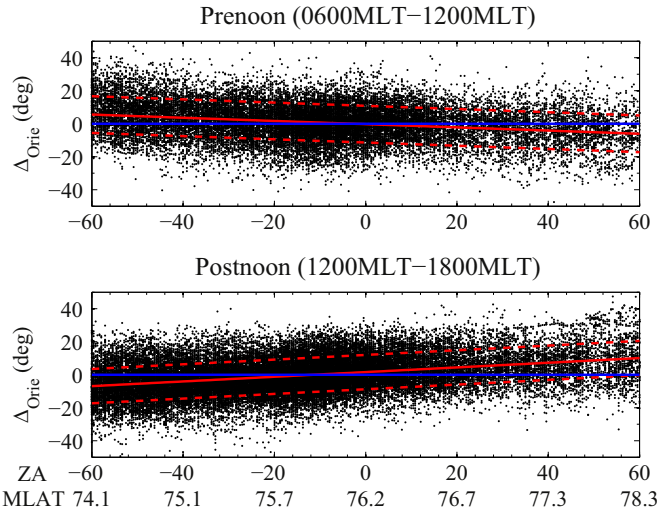

Fig. 3. Arc tilt as a function of ZA (MLAT) in the prenoon and postnoon sectors. Best fit linear regression lines are plotted with solid red lines and ± 1 σ deviation from linear regression line are plotted with dashed red lines. (For interpretation of the references to color in this figure, the reader is referred to the web version of this article.)

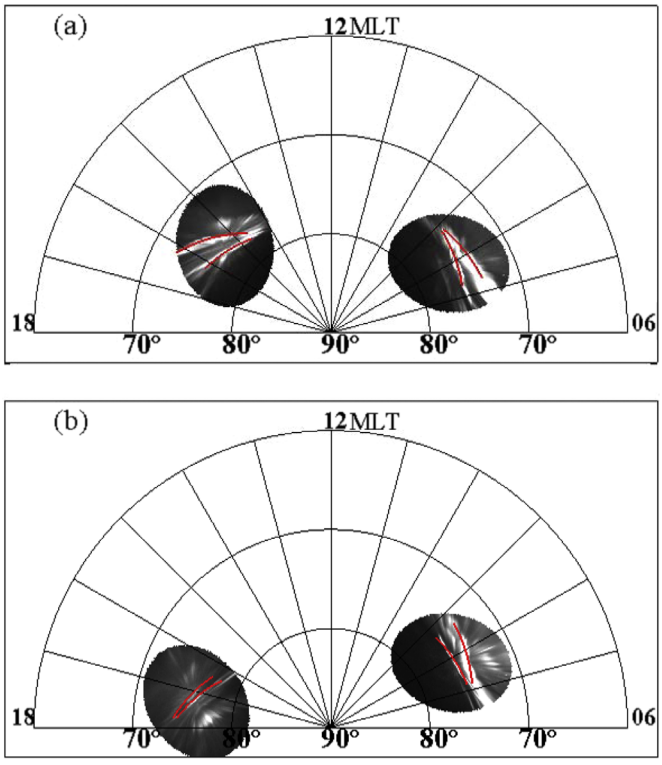

Fig. 4. The examples of multiple arcs plotted in the MLT-MLAT coordinates.

10.5 MLT.

The variation of arc orientation in magnetic latitude is plotted in Fig. 3. We used Δ_{orie} to reduce the longitudinal effect. Δ_{orie} is the deviation value between arc orientation and the mean orientation at that time. The top and bottom panels are scatter plots of Δ_{orie} as a function of ZA in the prenoon and postnoon sectors, respectively. The best fit linear regression line is plotted with solid red line. From Fig. 3, there is a clear trend between Δ_{orie} and latitude. The average Δ_{orie} decreases from 5.6° at −60° of ZA (74.1 MLAT) to −6.1° at 60° of ZA (78.3 MLAT) in the prenoon sector, but it increases from −7.0° to 10.1° in the postnoon sector. Positive Δ_{orie} means the arc alignment tilted to evening side relative to the average orientation at that time, and negative Δ_{orie} means arc alignment tilted to morning side. Thus, the arc alignment tilts to morning side in the higher latitude and tilts to evening side in the lower latitude in the prenoon sector, whereas it is the opposite in the postnoon sector. Arc tilt φ is zero at the reversal point. Because arc orientation ψ is larger in the lower latitude in the prenoon sector, it is found that the MLT at the reversal position is larger using (Eqs. (3) and 4). Thus, the tilt reversal point will shift closer to the midday in the lower latitude.

Fig. 4a shows two multiple-arc examples satisfied the dependence of the arc orientation on MLAT. We can see multiple arcs converge to a point near magnetic midday whether in the prenoon or postnoon sector. There are 5346 multiple-arc images (78%) and 9641 images (77%) are similar to examples in Fig. 4a in the prenoon and postnoon sectors, respectively. We also found some different events (Fig. 4b) that the intersections of multiple arcs are near dawn and dusk in the prenoon and postnoon sectors, respectively. Due to magnetic field lines converged on cusp in the midday sector, the magnetospheric source region of auroral arcs is narrower as it is closer to midday. Maybe that is why most of multiple arcs converged near magnetic midday.

Fig. 5 shows each arc alignment for each image. The equatorward (poleward) tilt of auroral arcs are plotted in blue (red). We can see most of arc tilts is poleward in the prenoon sector and the

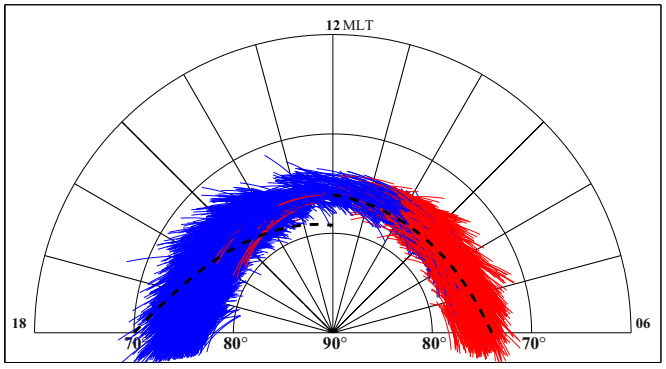

Fig. 5. The orientation of auroral arc as a function of MLT and MLAT. The equatorward (poleward) tilts of auroral arcs are shown in blue (red). The mean orientation of auroral arc as a function of MLT is plotted with dashed line. (For interpretation of the references to color in this figure, the reader is referred to the web version of this article.)

opposite arc alignment behavior in the postnoon sector. This is in agreement with what was shown in Fig. 2b. The dashed lines shows the mean orientation of auroral arc as a function of MLT. The latitude crossed over by arc alignment is 2.1° from dawn to midday. But it is larger (9.1°) from midday to dusk. That is because the mean arc tilt turns from poleward to equatorward in the prenoon sector, nevertheless, it is always equatorward and the absolute value is larger in the postnoon sector. From Fig. 5, we can see the MLT variation of mean auroral arc orientation is similar to that of the distribution of upward field-aligned current (FAC) obtained by Iijima and Potemra (1976). Auroral emission produced by downward electron flux is associated with an upward FAC over the arc (Aikio et al., 2002; Kozlovsky et al., 2009). This current is closed by a transverse Pedersen current in the ionosphere, and a return downward FAC is adjacent to the arc.

Since auroral particles are precipitated along magnetic field line, IMF should play an important role in the formation of auroral arcs. The IMF conditions we used is the OMNI data. In 4 year

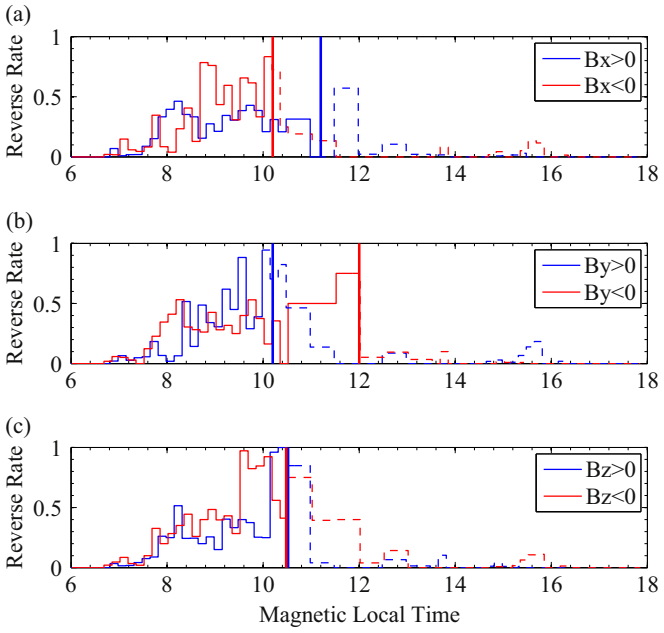

Fig. 6. Distributions of MLT of arc tilt reverse rate with different (a) IMF B_x, (b) B_y and (c) B_z components. The blue (red) lines are in the condition of positive (negative) IMF component. The thick vertical lines represent the arc tilt reversal positions. (For interpretation of the references to color in this figure, the reader is referred to the web version of this article.)

period, the mean IMF B_x, B_y and B_z components are 0.3, −0.3 and 0.2 nT, respectively. Fig. 6 shows the distributions of the reverse rate of arc tilt with different IMF conditions against MLT. The reversal points are labeled with vertical lines, which are plotted in blue and red from top to bottom panel in Fig. 6 for the positive and negative IMF B_x, B_y or B_z components respectively. Due to the lack of data between 11.0 and 11.5 MLT for positive B_x, the reverse rate is zero in Fig. 6a. But we can see the reverse rates are poleward and equatorward before 11.0 and after 11.5 MLT, respectively, and the peak value is much less than 1.0. It can be conjectured that the mean reversal point is located at about 11.3 MLT (the center between 11.0 and 11.5 MLT), which is closer to the midday. The mean reversal location for negative B_x is approximately 10.2 MLT, which is closer to dawn. We can also find the arc tilt reversal position shifts to the midday for negative B_y, which is shown by the solid red line at 12.0 MLT in Fig. 6b. From Fig. 6c, the influence on arc tilt reversal point with IMF B_z component is not obvious.

Through investigation of IMF effects, we find some interesting results. Positive B_x and negative B_y tend to shift the reversal point toward the midday, whereas negative B_x and positive B_y shift it toward the dawn. For negative B_y, the cusp-related field-aligned currents (midday region 1) shift dawnward, connected to region 2 field-aligned current in the prenoon sector (Watanabe et al., 1996). Upward field-aligned currents extend from prenoon sector to postnoon sector (McDiarmid et al., 1979). From Fig. 3 in Chisham et al.'s study, we see statistical patterns of ionospheric convection for different IMF clock angle orientations (Chisham et al., 2007). We can find the convection cells tilt to evening (morning) side for negative (positive) B_y. For positive B_y, just like convection in ionosphere, the alignment of auroral arc tilts to the morning side. Arc orientation is decreased as the arc tilts to the morning side and it will result in a shift of the reversal point toward the dawn. Whereas the arc tilts to the evening side and the reversal position shifts toward the midday with negative B_y. Due to the Parker spiral structure of the IMF (Parker and Jokipii, 1976), the shift of reversal position influenced by IMF B_x only follows the IMF B_y effect. In this study, the mean IMF B_y is 2.0 nT when $B_x < 0$, whereas it is −1.9 nT when $Bx > 0$. Thus, the IMF By is the main factor controlling the arc orientation.

4. Conclusions

We surveyed over 40,000 dayside auroral arc ASIs observed at YRS during a 4 year period demonstrating a regular variation of the orientation of dayside auroral arc alignments. The conclusions of this study can be summarized as follows:

1. The orientation variation of dayside auroral arc alignments is presented a clear tendency as a function of MLT. The mean reversal point of arc tilt is near 10.5 MLT.
2. Compared with the mean orientation, auroral arc alignment tilts to morning side in the higher latitude and tilts to evening side in the lower latitude in the prenoon sector, whereas it is the opposite in the postnoon sector. The reversal point will be closer to the midday in the lower latitude.
3. The IMF B_y component plays an important role in the location of the arc tilt reversal point. Negative B_y will shift the position of the reversal point closer to the midday.

The orientation of dayside auroral arc alignment is closely related to the distribution of field-aligned current. The effect of the IMF is to change the earth's magnetic field to influence the distribution of field-aligned current. The motion of auroral arc may also have an impact on its orientation. The motion characteristics of dayside auroral arcs will be investigated in the future.

Acknowledgments

This work was supported by the National Natural Science Foundation of China (41431072, 41374161, 41274164, 41374159, 41304149 and 41504115), the Polar Environment Comprehensive Investigation and Assessment Programs (CHINARE 2016-02-03, 2016-04-01), the Pudong Development of Scientific and Technology Program (PKC2013-207). Thanks are also given for the Strategic Priority Research Program on Space Science, Chinese Academy of Sciences (XDA04060201) and the Shaanxi province Natural Science Foundation (2015JQ6223). This work was supported by the Top-Notch Young Talents Program of China, and the International Collaboration Supporting Project, Chinese Arctic and Antarctic Administration (IC201608). We acknowledge the NASA OMNIWeb site to supply the IMF data.

References

Aikio, A.T., Lakkala, T., Kozlovsky, A., Williams, P.J.S., 2002. Electric fields and currents of stable drifting auroral arcs in the evening sector. J. Geophys. Res. 107 (A12), 1424.
Borovsky, J.E., 1993. Auroral arc thicknesses as predicted by various theories. J. Geophys. Res. 98 (A4), 6101–6138.
Chisham, G., lester, M., Milan, S.E., et al., 2007. A decade of the Super Dual Auroral Radar Network (SuperDARN): scientific achievements, new techniques and future directions. Surv. Geophys. 28 (1), 33–109.
Cogger, L.L., Murphree, J.S., Ismail, S., Anger, C.D., 1977. Characteristics of Dayside 5577Å and 3914 Å Aurora. Geophys. Res. Lett. 4 (10), 413–416.
Davis, T.N., 1978. Observed characteristics of auroral forms. Space Sci. Rev. 22 (1), 77–113.
Feldsten, Y.I., 1963. Some problems concerning the morphology of auroras and magnetic disturbances at high latitudes. Geomagn. Aeron. 3, 183–192.
Feldsten, Y.I., Starkov, G.V., 1967. Dynamics of auroral belt and polar geomagnetic disturbances. Planet. Space Sci. 15 (2), 209–229.
Gillies, D.M., Knudsen, D.J., Donovan, E.F., Spanswick, E.L., Hansen, C., Keating, D., Erion, S., 2014. A survey of quiet auroral arc orientation and the effects of the interplanetary magnetic field. J. Geophys. Res. 119 (4), 2550–2562.
Hu, Z.-J., Yang, H., Huang, D., Araki, T., Sato, N., Taguchi, M., Seran, E., Hu, H., Liu, R., Zhang, B., 2009. Synoptic distribution of dayside aurora: multiple-wavelength all-sky observation at Yellow River Station in Ny-Ålesund, Svalbard. J. Atmospheric Sol.-Terr. Phys. 71 (8-9), 794–804.
Hultqvist, B., 1962. On the orientation of auroral arcs. J. Atmos. Terr. Phys. 24 (1), 17–30.
Iijima, T., Potemra, T.A., 1976. Field-aligned currents in the dayside cusp observed by Triad. J. Geophys. Res. 81 (34), 5971–5979.
Kozlovsky, A., Kangas, J., 2002. Motion and origin of noon high-latitude poleward moving auroral arcs on closed magnetic field lines. J. Geophys. Res. 107 (A2), 1017.
Kozlovsky, A., Turunen, T., Massetti, S., 2009. Field-aligned currents of postnoon auroral arcs. J. Geophys. Res. 114, A03301.
Lassen, K., Danielsen, C., 1978. Quiet time pattern of auroral arcs for different directions of the interplanetary magnetic field in the Y–Z plane. J. Geophys. Res. 83 (A11), 5277–5284.
Liou, K., Newell, P.T., Meng, C.I., Brittnacher, M., Parks, G., 1997. Synoptic auroral distribution: a survey using polar ultraviolet imagery. J. Geophys. Res. 102 (A12), 27197–27205.
McDiarmid, I.B., Burrows, J.R., Wilson, M.D., 1979. Large-scale magnetic field perturbations and particle measurements at 1400 km on the Dayside. J. Geophys. Res. 84 (A4), 1431–1441.
Newell, P.T., Lyons, K.M., Meng, C.I., 1996. A large survey of electron acceleration events. J. Geophys. Res. 101 (A2), 2599–2614.
Parker, G.D., Jokipii, J.R., 1976. The spiral structure of the interplanetary magnetic field. Geophys. Res. Lett. 3:9 (9), 561–564.
Qiu, Q., Yang, H.-G., Lu, Q.-M., Zhang, Q.-H., Han, D.-S., Hu, Z.-J., 2013. Widths of dayside auroral arcs observed at the Chinese Yellow River Station. J. Atmospheric Sol.-Terr. Phys. 102, 222–227.
Sandholt, P.E., Carlson, H.C., Egeland, A., 2002. Dayside and Polar Cap Aurora. Kluwer Academic Publishers, Dordrecht, pp. 9–28.
Watanabe, M., Iijima, T., Rich, F.J., 1996. Synthesis models of dayside field-aligned currents for strong interplanetary magnetic field By. J. Geophys. Res. 101 (A6), 13303–13319.